Numerical Simulations of a 2D Stratified Shear Layer with Comparison to Predictions from Linear Stability Theory

Matt de Stadler
June 8, 2008

Introduction

In this paper results from a 2D stratified shear layer simulation are compared with those from Hazel's 'Numerical studies of the stability of inviscid stratified shear flows'. Evaluation and comparison of the wavelength of the most unstable mode and its growth rate were made for different Reynold's numbers, Bulk Richardson numbers, and initial perturbation profiles. The results from these test cases were compared with each other and with the prediction of Hazel. The question of whether linear stability theory could provide an insight into the time of pairing was investigated numerically.

Problem Statement

We consider a parallel shear flow with a continuous velocity and temperature distribution. After applying the Boussinesq approximation and non-dimensionalizing we obtain the following dimensionless governing equations.

$$\nabla \cdot u = 0$$
$$\frac{\partial u}{\partial t} + u \cdot \nabla u = -\nabla p + \frac{1}{\mathrm{Re}} \nabla^2 u + Ri_b (T - T_0)$$
$$\frac{\partial T}{\partial t} + u \cdot \nabla T = \frac{1}{\mathrm{Re}\,\mathrm{Pr}} \nabla^2 T$$

Where

$$\mathrm{Re} = \frac{\delta_{w,0} \Delta U}{\nu}$$
$$Ri_b = \frac{g \alpha \Delta T \delta_{w,0}}{(\Delta U)^2} = -\frac{g \Delta \rho \delta_{w,0}}{\rho_0 (\Delta U)^2}$$
$$\mathrm{Pr} = \frac{\nu}{\kappa}$$

The other variables are defined in the figure below or else according to standard convention.

Figure 1. Velocity and Temperature Profiles for the Base State

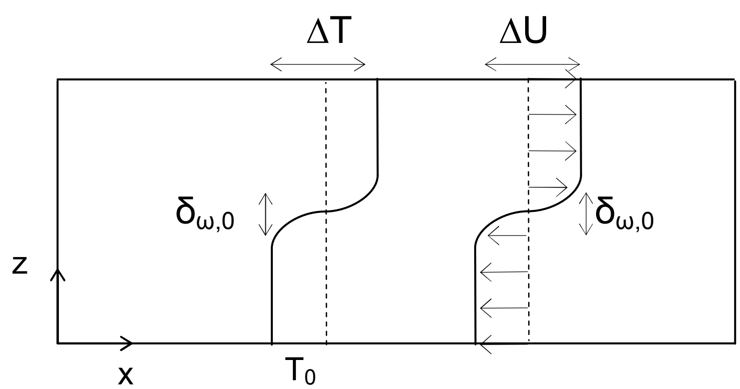

Initial Conditions

The simulations were conducted using tanh profiles as shown in Figure 1; their equations are given below

$$u = \tanh\left(\frac{2y}{\delta_{\omega,0}}\right)$$

$$T - T_0 = \tanh\left(\frac{2y}{\delta_{\omega,0}}\right)$$

$$p = 0$$

$$\delta_{\omega,0} = 1$$

The initial pressure distribution is chosen for convenience and is not physically true. However, it is quickly updated by the pressure solver to nearly match a hydrostatic profile. The scaling for the temperature is slightly different in this case and that of Hazel.

Initial Perturbations

Three different profiles were used for the perturbations, a random distribution over the shear layer, an ordered distribution designed to set off the most unstable mode from linear stability theory (called the primary mode in the rest of this paper), and an ordered distribution to set off a wavelength of twice the primary mode.

The equations used for these perturbations are given below, along with contour plots showing their initial shape.

Random perturbations

$$u' = w' = \hat{u} \cdot rand(0-1)\exp\left(\frac{z}{2\delta_{\omega,0}}\right)$$

Ordered perturbations

$$u' = \hat{u} \cdot \sin\left(\frac{2\pi k_x x}{L}\right)\exp\left(\frac{|z|}{\delta_{\omega,0}}\right)$$

$$w' = \hat{w} \cdot \sin\left(\frac{2\pi k_x x}{L}\right)\exp\left(\frac{|z|}{\delta_{\omega,0}}\right)$$

Where k_x represents the number of wavelengths in the domain, a value of 2 corresponds to the most unstable mode and a value of 1 corresponds to twice the wavelength of the most unstable mode. Negative 1 was used for k_x in the twice the wavelength of the most unstable mode case so that resulting Kelvin-Helmholtz rollers would be in the center and not on the side of the domain.

This is purely for convenience in viewing the results. The perturbation strengths are given by $\hat{u}$ and $\hat{w}$, they are chosen to be equal.

Figure 2. Perturbation Structure

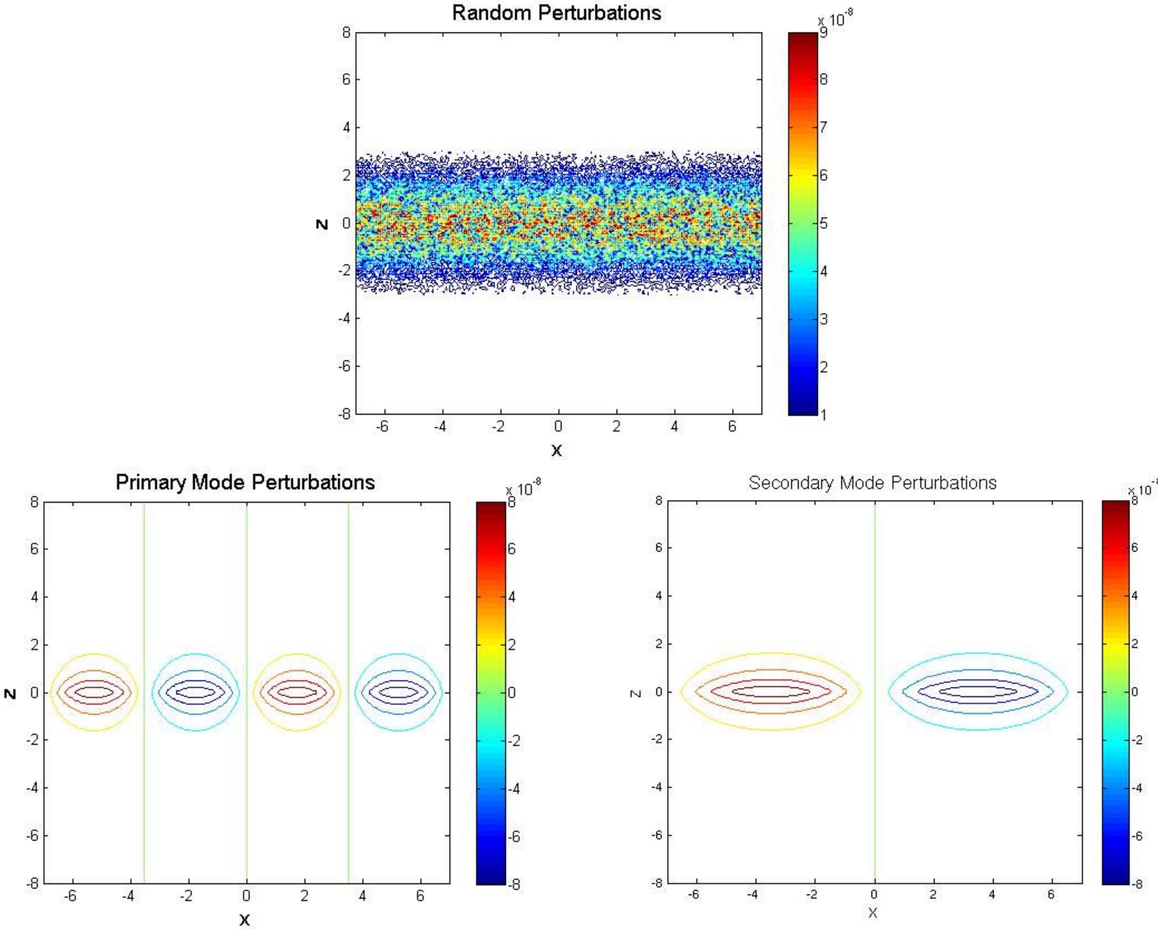

It is important to note that the perturbations added above are not filtered to be divergence free and hence the simulations begin with initial divergence.

Simulation setup

All the simulations were run with the following parameters

Table 1. Simulation settings

Horizontal domain size	14
Vertical domain size	16
x grid points	180
y grid points	210
Perturbation Strength	10^{-7}
Final t_{growth} (unstratified)	26
Final t_{growth} (stratified)	44
Order of accuracy (space and time)	2

The domain size was chosen to correspond to twice the wavelength of the primary mode in the horizontal direction. The vertical domain size was chosen to allow the shear layer to develop without interference from the boundaries. The perturbation strength was chosen to be very small in accordance with the requirements of linear stability theory.

The following boundary conditions were applied at the top and bottom boundaries; they represent far field conditions to allow the simulation to develop in the absence of walls. The variables below are dimensionless.

$$\frac{\partial^2 u}{\partial y^2} = \frac{\partial^2 w}{\partial y^2} = 0, \frac{\partial \rho}{\partial y} = \frac{\partial T}{\partial y} = 0, \frac{\partial p}{\partial y} = 0$$

The simulation is periodic in the x-direction.

A total of 12 runs were performed. Three parameters were varied for each run, the Reynolds number, the Bulk Richardson number and the structure of the initial perturbations.

Results from Linear Stability Theory

Hazel obtained a prediction for the wavelength of the fastest growing mode along with a prediction for the growth rate. He obtained these results from the non-dimensional Taylor-Goldstein equation. Below is the dimensional form.

$$\frac{d^2 w}{dz^2} + \left(\frac{N^2(z)}{\left(U(z) - C\right)^2} - \frac{d^2 U / dz^2}{U(z) - C} - k^2 \right) w(z) = 0$$

Where w(z) is a single Fourier component of the vertical perturbation velocity, z is the vertical coordinate, N(z) is the local Brunt-Väisälä frequency given by $N^2(z) = -g(d\rho/dz)/\rho$; U(z) is the base state velocity profile and C is the complex phase speed of the wave mode of wavenumber k. This equation is valid for small disturbances in an inviscid, incompressible, stratified, parallel shear flow with the Boussinesq approximation. Hazel non-dimensionalized his equation, see paper for details, to obtain the dimensionless Taylor-Goldstein equation.

$$\frac{d^2 \phi}{dy^2} + \left(\frac{J\beta'}{\left(u - c\right)^2} - \frac{d^2 u / dy^2}{u - c} - \alpha^2 \right) \phi(y) = 0$$

This equation allows one to obtain the growth rate αc_i, and the most unstable mode, α for a given Richardson number J. The following chart was obtained for profiles with u = tanh(y) and β = tanh(y).

Figure 3. Hazel's Solution.

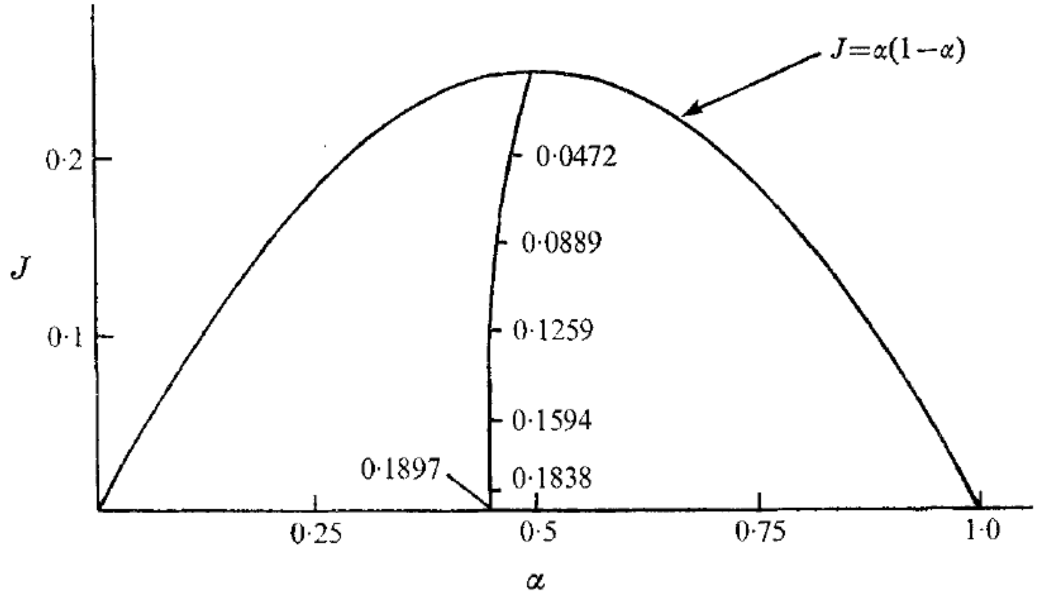

FIGURE 1. Stability boundary and curve of maximum growth rate for 'tanh' profiles, with growth rates marked.

Results

The values in the following table were obtained using cg, Overture's Navier Stokes solver.

Table 2. Simulation results.

Re	Ri_b	Perturbations	Time for roll up	Time for pairing (+/- 3)	Growth rate
500	0	Random noise	88* (2nd mode)	n/a	0.251
500	0	Primary mode	68	n/a	0.306
500	0	Secondary mode	69	n/a	0.275
500	0.05	Random noise	98* (2nd mode)	n/a	0.214
500	0.05	Primary mode	96	n/a	0.182
500	0.05	Secondary mode	78	n/a	0.200**
2000	0	Random noise	63	82	0.337
2000	0	Primary mode	48	n/a	0.354
2000	0	Secondary mode	61	n/a	0.292
2000	0.05	Random noise	67	88	0.250
2000	0.05	Primary mode	53	n/a	0.292
2000	0.05	Secondary mode	68	n/a	0.240

The wavelength of the initial roll-up was observed to be ≈ 7 for the primary mode and ≈ 14 for both the secondary mode and pairing.

The values in the following table correspond to results from Hazel shown in Figure 3.

Table 3. Hazel's predicted values from linear stability theory.

Re	Ri	Growth rate
∞	0	0.422-0.431
∞	0.5	0.354-0.362

The wavelength of the most unstable mode is predicted to be ≈ 7 for both the stratified and unstratified case.

Measuring the growth rate

To get an estimate of the growth rate, it was necessary to determine a measure to describe the time evolution of the perturbation. Since the Taylor Goldstein equation governs the behavior of the vertical velocity perturbation, the vertical velocity was used to determine the growth rate. This calculation was simplified by the fact that the base state has zero vertical velocity; therefore each vertical velocity measurement is equal to the vertical velocity perturbation.

The vertical velocity was measured at three points, z = -0.498, z = -0.038 and z = 0.421. This gives one point at the center of the shear layer and two points near the initial edge of the shear layer. The shear layer diffuses outward over time so these points do not remain near the boundary. At each of these locations a line average is taken of the square root of the square of the vertical velocity.

$$< w >= \frac{\sum_{i=1}^{N_x} \sqrt{w_i^2}}{N_x}$$

The three values of <w> are then plotted over time as shown below in Figures 4(a) and 5(a). The real part of the growth rate is proportional to exp(st). By plotting t vs. ln (<w>) as shown below in Figures 4(b) and 5(b), the value of s can be determined by a linear fit for each z location. The overall growth rate was then taken to be the average of the growth rate at each of the z locations.

Figure 4. Unstratified Growth Rate

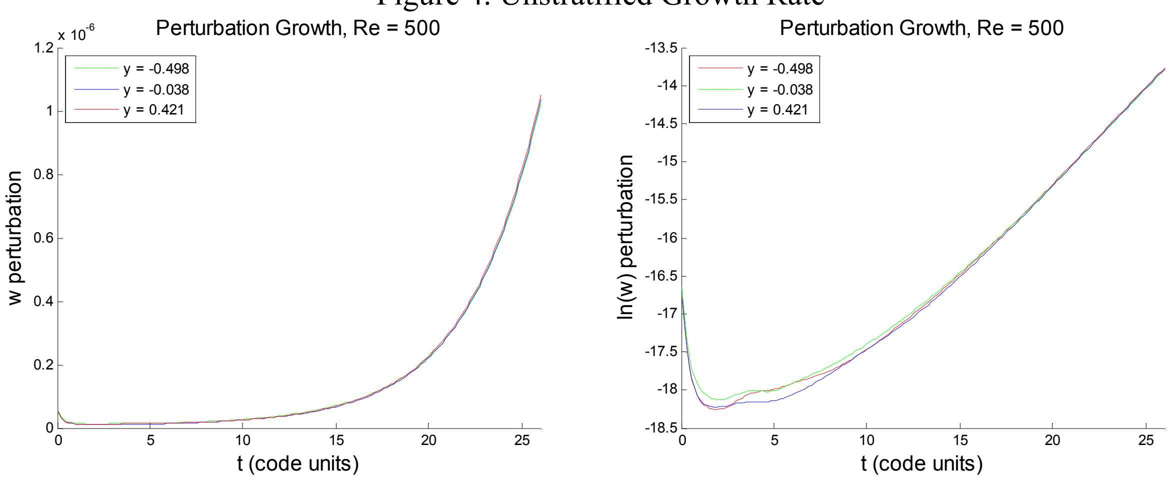

(a) Perturbation evolution in time (b) ln(perturbation) vs. time

Figure 5. Stratified Growth Rate

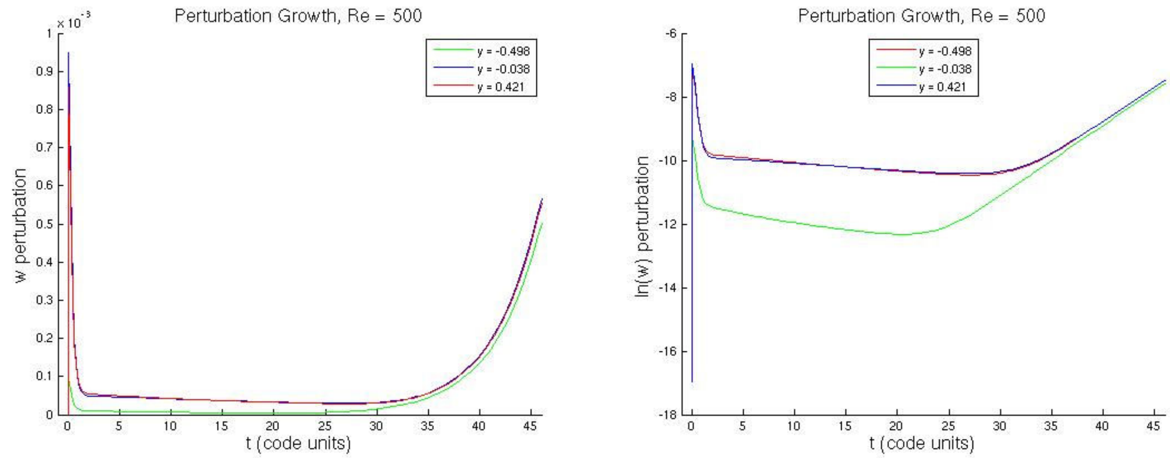

(a) Perturbation evolution in time. (b) ln(perturbation) vs. time.

Observing Roll-up and Pairing

It is clear that vortex rollers form in the flow but it is difficult to give a qualitative estimate of their time of formation. The same is true for pairing. One has several options for how to define each of these times. For the data reported above, the time for roll up was defined to be the time that the first sharp corner formed in the vortex as shown below in Figure 5. The same convention was used for pairing. Another possible option is to use the time that the initial perturbations reach finite amplitude as shown in Figure 6.

Figure 6. Initial perturbations at finite amplitude

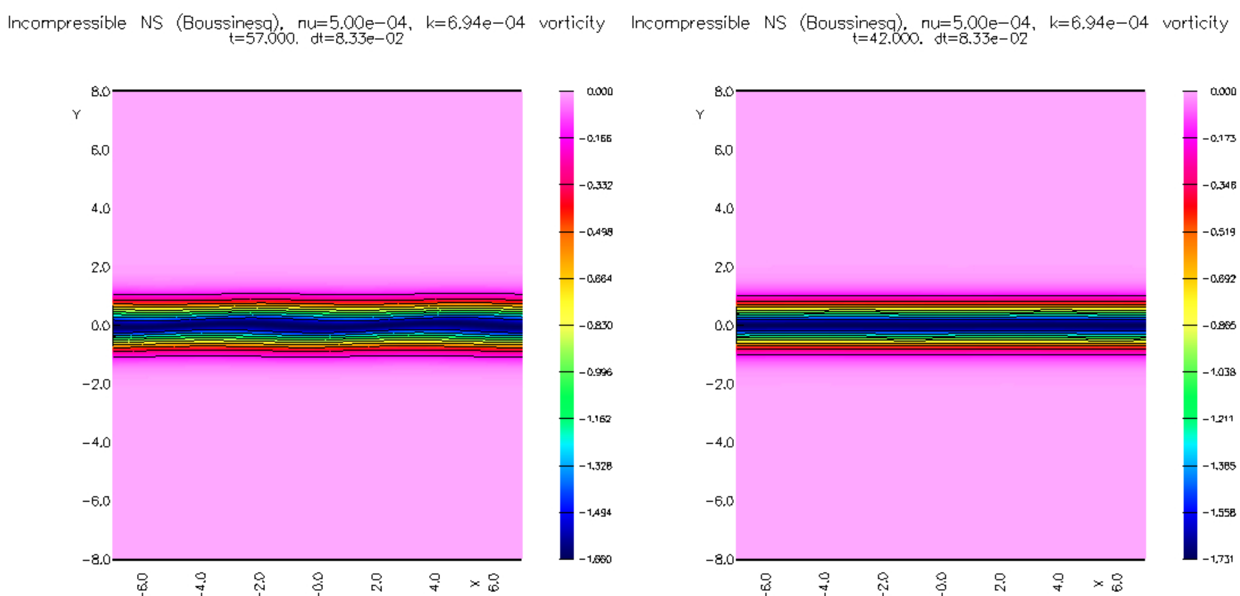

(a) Stratified case. (b) Unstratified case.

Figure 7. Initial Roll-up

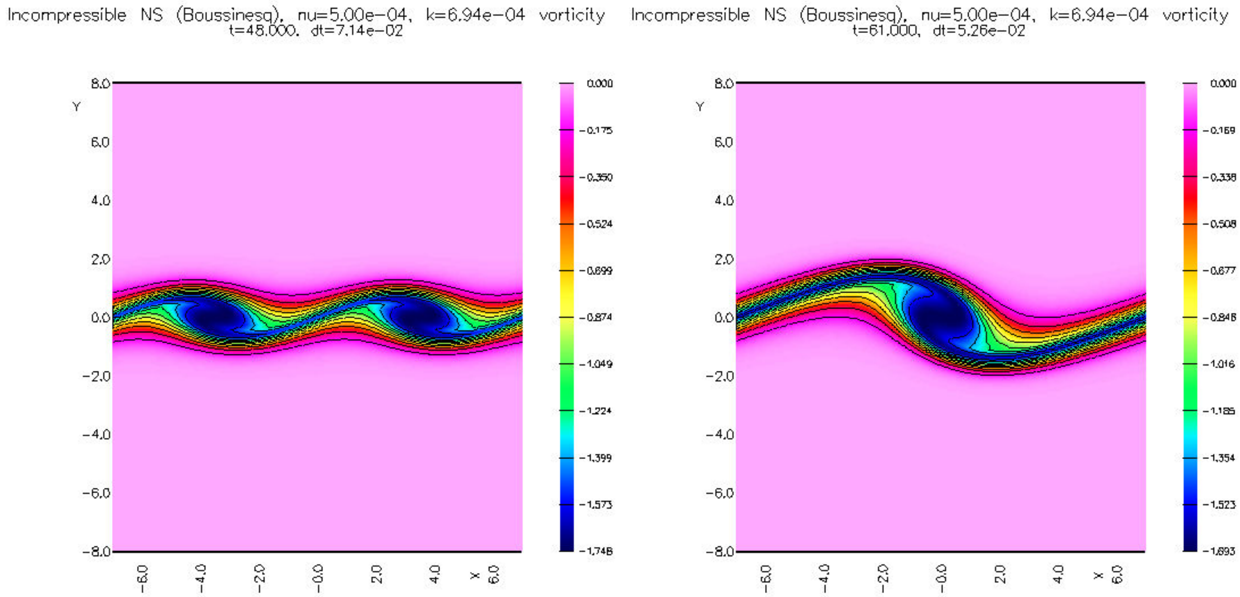

(a) Most unstable mode

(b) Twice the wavelength of the most unstable mode

Figure 8. Pairing

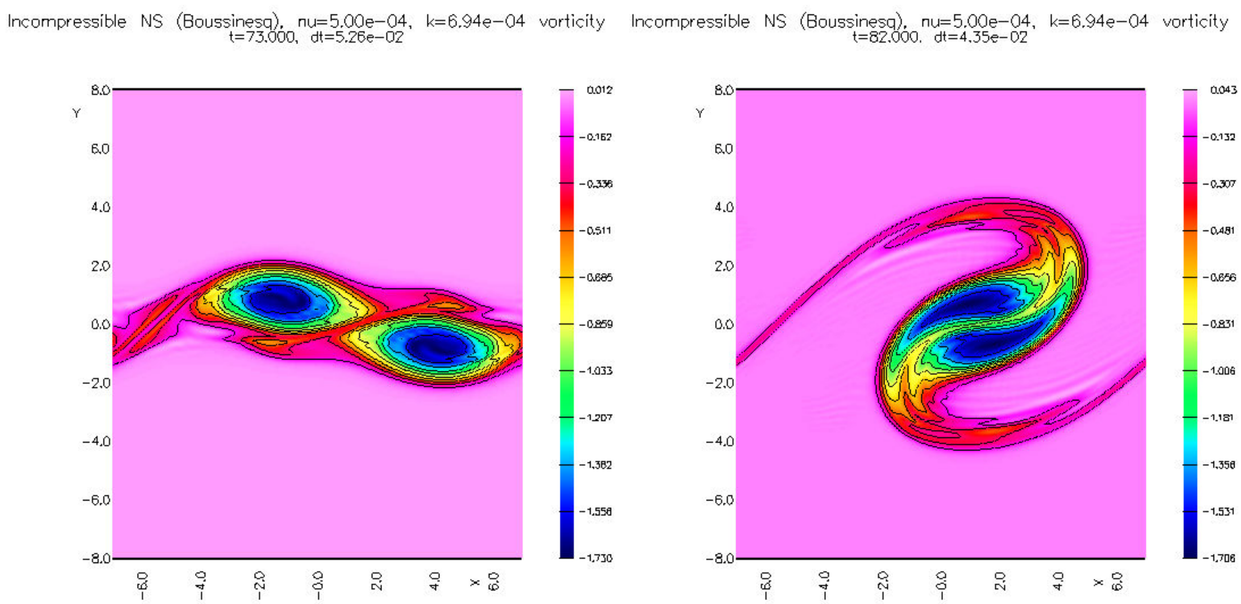

(a) Early pairing.

(b) Fully paired.

Discussion of Results

Linear stability theory does a good job predicting the unstable nature of the flow system. The prediction of growth rate is reasonably well approximated, and it improves as viscosity is reduced. The wavelength of the first rollers is in excellent agreement with that predicted by linear stability theory for cases with low viscosity. For higher viscosities the predictions are not very good. Another cause of discrepancies between the observed results and those of Hazel is that the density (Hazel) and temperature (this paper) profiles are scaled in a slightly different way.

Four observations can be made from the simulations results table.

1. Viscosity reduces growth rates and damps low wavelength solutions
2. Buoyancy reduces growth rates
3. In 3 of the cases the time of rollup for the random perturbations agrees well with the time of formation for the slower wavelength but exhibits the structure of the faster growing wavelength
4. For higher Re, initial growth rate is a good predictor of what mode will appear first

The first result above is to be expected and the effect is most pronounced in the Re = 500 cases. Despite the relatively highly viscous nature of these cases, the growth rate is within fifty percent of that predicted by the inviscid theory of Hazel. The Re = 2000 case is within seventy five percent of Hazel's predicted value which lead one to believe that for even higher Re values, the agreement would improve. The greater grid resolution needed to resolve higher Re simulations, and hence greater computing time required, prevented testing of this hypothesis for this paper.

The second result is also expected as buoyancy acts as a restoring force to this system. The effect of buoyancy appears to be much greater for the lower wavelength case. This can be seen in the difference in the time of formation of the primary mode for ordered perturbations between the Re = 500, $Ri_b = 0.0$ and the Re = 500, $Ri_b = 0.05$ case.

The third result is very interesting and unexpected. The cases with random perturbations showed strange correlation with the cases of ordered perturbations to target the primary instability and the secondary instability. The fastest growing mode from the ordered perturbations cases was the one found to occur in the random perturbations case. It is very surprising to observe that the time for this to occur agrees extremely well with the slower of the two growing modes for a given case. While one expects the results of the random perturbations case to differ from those of the ordered perturbations case due to the broadband nature of the initial perturbations, one does not expect to see such good agreement in the time of formation between the random case and the slower of the two ordered modes. It is even stranger to note that the structure of the faster growing mode occurs instead of the structure of the slower mode.

The fourth result is to be expected and agrees well with the predictions of linear stability theory.

From the growth rate figures, four observations can be made

1. After initial oscillations, exponential growth occurs
2. Stratification reduces the time that exponential growth begins to dominate
3. Perturbations grow in a different manner at different z locations

The behavior of the perturbations as shown in Figures 4 and 5 agrees well with the existence of a normal mode solution. There is clearly a combination of initial perturbations and exponential growth. This can be seen most easily in Figure 4b.

There is a large difference in the time that it takes for exponential growth to occur in the stratified and unstratified cases. The stratified case takes about three times as long as the unstratified case to show exponential growth. The initial spike in the stratified profile is likely due to the pressure correction from the poisson pressure solver. Since the initial conditions are not a true solution to the Navier-Stokes equations (p is set to zero initially) it will take a few iterations before the code will correct for this. Divergence damping also likely affects this start time. Even with these two effects, it is observed that the exponential growth begins to dominate at a much later time. It would be instructive to start the simulation as a solution to the N-S equations and then observe how much the time of exponential growth differs.

At different z locations within the shear layer, the perturbations behave differently. This is most clearly seen by looking at Figures 4b and 5b. The differences are most pronounced in the stratified case.

There appears to be no correlation between the time of pairing and the time for the roller for the secondary mode to form. Once the primary rollers form the flow is already highly non-linear and the corresponding vortex interaction can not be predicted by linear stability theory.

Conclusion

These simulations show mixed agreement with the results of linear stability as found by Hazel. As these simulations were run at a viscosity large enough to violate the inviscid assumption for the Taylor-Goldstein equation, the agreement between the theory and the observed results is actually quite good for the wavelength of the most unstable mode. The growth rate is reasonably approximated in the Re = 2000 cases. However, the time of formation of the rollers and their structure as described in conclusion 3 from the simulation results table is very strange and should be investigated further. No correlation between the time of pairing and the time of rollup for the secondary mode was obtained. A better comparison between the stratified results and Hazel's prediction would be obtained for a temperature profile matching the one used by Hazel. A better test of the theory would be to significantly increase the Reynolds number and then compare the results obtained to those of Hazel.

References

Philip Hazel (1972). Numerical studies of the stability of inviscid stratified shear flows. *Journal of Fluid Mechanics Digital Archive,* **51**, pp 39-61.

cg/Overture
https://computation.llnl.gov/casc/Overture/